

A Model Predictor for Chemical Laser Combustors

15 December 2001

Prepared by

M. A. KWOK
Space-Based Laser
Space Support Division

Prepared for

SPACE AND MISSILE SYSTEMS CENTER
AIR FORCE SPACE COMMAND
2430 E. El Segundo Boulevard
Los Angeles Air Force Base, CA 90245

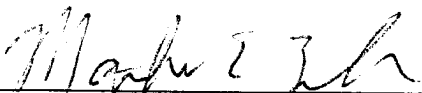
20020514 137

Space Systems Group

This report was submitted by The Aerospace Corporation, El Segundo, CA 90245-4691, under Contract No. F04701-00-C-0009 with the Space and Missile Systems Center, 2430 E. El Segundo Blvd., Los Angeles Air Force Base, CA 90245. It was reviewed and approved for The Aerospace Corporation by K. P. Zondervan, Systems Director, Space-Based Laser. Capt. Matthew Zuber was the project officer for the program.

This report has been reviewed by the Public Affairs Office (PAS) and is releasable to the National Technical Information Service (NTIS). At NTIS, it will be available to the general public, including foreign nationals.

This technical report has been reviewed and is approved for publication. Publication of this report does not constitute Air Force approval of the report's findings or conclusions. It is published only for the exchange and stimulation of ideas.



Capt. Matthew Zuber
SMC/TLS

REPORT DOCUMENTATION PAGE

Form Approved
OMB No. 0704-0188

Public reporting burden for this collection of information is estimated to average 1 hour per response, including the time for reviewing instructions, searching existing data sources, gathering and maintaining the data needed, and completing and reviewing this collection of information. Send comments regarding this burden estimate or any other aspect of this collection of information, including suggestions for reducing this burden to Department of Defense, Washington Headquarters Services, Directorate for Information Operations and Reports (0704-0188), 1215 Jefferson Davis Highway, Suite 1204, Arlington, VA 22202-4302. Respondents should be aware that notwithstanding any other provision of law, no person shall be subject to any penalty for failing to comply with a collection of information if it does not display a currently valid OMB control number. PLEASE DO NOT RETURN YOUR FORM TO THE ABOVE ADDRESS.

1. REPORT DATE (DD-MM-YYYY) 15-12-2001		2. REPORT TYPE		3. DATES COVERED (From - To)	
4. TITLE AND SUBTITLE A Model Predictor for Chemical Laser Combustors				5a. CONTRACT NUMBER F04701-00-C-0009	
				5b. GRANT NUMBER	
				5c. PROGRAM ELEMENT NUMBER	
6. AUTHOR(S) M. A. Kwok				5d. PROJECT NUMBER	
				5e. TASK NUMBER	
				5f. WORK UNIT NUMBER	
7. PERFORMING ORGANIZATION NAME(S) AND ADDRESS(ES) The Aerospace Corporation Space Systems Group El Segundo, CA 90245-4691				8. PERFORMING ORGANIZATION REPORT NUMBER TR-2001(1019)-2	
9. SPONSORING / MONITORING AGENCY NAME(S) AND ADDRESS(ES) Space and Missile Systems Center Air Force Space Command 2430 E. El Segundo Blvd. Los Angeles Air Force Base, CA 90245				10. SPONSOR/MONITOR'S ACRONYM(S) SMC	
				11. SPONSOR/MONITOR'S REPORT NUMBER(S) SMC-TR-02-23	
12. DISTRIBUTION/AVAILABILITY STATEMENT Approved for public release; distribution unlimited.					
13. SUPPLEMENTARY NOTES					
14. ABSTRACT This spreadsheet model attempts to replicate many of the empirical features observed in HF chemical laser combustors, or gain generators, from time-start. The model, dubbed HYFLAME, is constructed from control volume analyses of the combustor vessel that are described by modules depicting the simplified combustion thermochemistry, fluid mechanics for one-dimensional steady nozzle flow, chemical kinetics in frozen flow, simplified heat transfer analyses, and a simple thermal-structural model. Model outputs include combustor plenum pressures, combustor stagnation temperatures, combustor core temperatures, and average temperatures of the vessel walls. The model's principal value is to compute a key laser performance parameter, the time dependent F-Atom flow rate $\dot{m}F$, which cannot be easily measured. Other equally elusive performance variables are the degree of fluorine dissociation and heat flux loss to the vessel. This variable is computed as a function of time for the Alpha Laser HL911-003 case. In principle for the same combustor, the model can predicted the numerous performance variables, given a new set of reagent flow rates as inputs.					
15. SUBJECT TERMS Chemical lasers, HF lasers, Space-based lasers, High-power lasers, Combustors, Combustor models, Gain generator models, Reactive flow					
16. SECURITY CLASSIFICATION OF:			17. LIMITATION OF ABSTRACT	18. NUMBER OF PAGES 11	19a. NAME OF RESPONSIBLE PERSON Munson Kwok
a. REPORT UNCLASSIFIED	b. ABSTRACT UNCLASSIFIED	c. THIS PAGE UNCLASSIFIED			19b. TELEPHONE NUMBER (include area code) (310)336-5441

Contents

INTRODUCTION	1
CYLINDRICAL COMBUSTOR.....	2
HOT ANNULUS	3
Inflow.....	4
Losses to the Core	4
Net Heat Losses to the Vessel.....	4
Hot Annulus Interior	6
NOZZLE FLOW	7
CORE VOLUME	8
ANCHORING PARAMETERS	9
PRINCIPAL RESULT	9
CLOSURE	10
ACKNOWLEDGMENTS.....	10
REFERENCES	11

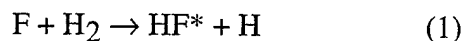
Figures

1. Combustor Wall Cross Section.....	2
2. HYFLAME Two Bin Model.....	2
3. Functional control volume diagram showing the overall Control Volume and the tyhree Control Sub-Volumes: Cold Core, Hot Annulus, Ring Nozzles.....	3
4. Typical result: A^* as $f(t)$ for HL911-003 case	6
5. Parameter f for HL911-003 case for $T_{e_{min}} = 1350^{\circ}K$	7
6. Fitting the P_c curve of HL911-003.....	8

7. Typical T_{Al} , T_{core} calculations, HL911-003	9
8. Families of HYFLAME Pc curves simulating HL911-003, to illustrate parameter anchoring	9
9. F-Atom Flow Rate computed from HYFLAME as a function of time.....	9
10. Computed degree of fluorine dissociation α for the HL911-003 flow conditions	10

INTRODUCTION

A key HF chemical laser performance variable is the flow rate of combustor-generated F-atoms, denoted \dot{m}_F , that reach the free jet laser medium. These atoms are in turn mixed with injected cavity fuel, hydrogen, to produce the excited HF molecules through the reaction



HF^* in turn produces the gain that can be coupled to a laser resonator. Thus in the crudest, simplest terms, the total laser power, say TP , that is generated is roughly proportional to the product of flow rates \dot{m}_F and cavity hydrogen \dot{m}_{H_2}

$$TP(t) = C \times \dot{m}_F \times \dot{m}_{H_2} \quad (2)$$

We return to this equation later. The need to better understand \dot{m}_F in Alpha Laser testing motivated the attempt to develop a model to deduce \dot{m}_F . That effort produced the previous report¹. Applying the assumption that temporal changes in combustor plenum pressure, P_c , were mainly due to changes in exit nozzle array throat gaps caused by thermal heating, an estimate for combustor heat loss could be made that in turn allowed an estimate of combustor performance, and, then, \dot{m}_F .

We quickly discovered that this first model was not usable at the earliest times after time-start because $P_c(t)$ changes were due mainly to the dynamics of increasing reagent flows and the onset of combustion. Thus the first model was really not useful as a predictor, which requires portrayal of the history of the combustor from time-start.

However, we found we could apply the methods and principles previously used. Namely, we would use control volume approach to formulate analyses of the combustor vessel. These analyses are described in modules depicting the combustion thermo-chemistry, fluid mechanics for one-dimensional steady nozzle flow, chemical kinetics for frozen flow, simplified conductive, radiative, and convective heat transfer analyses, and a simple portrayal of the vessel wall thermal-structural response. Moreover, we quickly discovered that creating a model of a cylindrical combustor from time-start would be more complex than expected.

Our goal remains a quick running personal computer type spreadsheet model, in which visibility of the simple-minded physics is always preserved. Spatial detailing is highly averaged or simplified. Our objective is to create a model usable for insight and understanding.

We will call our model HYFLAME, for “HYdrogen Fluoride Laser Aerospace Model in Excel®.”

CYLINDRICAL COMBUSTOR

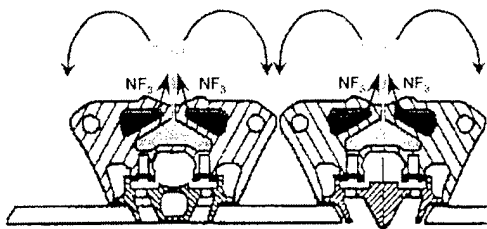


Fig. 1. Combustor Wall Cross Section

The Alpha Laser combustor is a clever design in which reagents are sprayed into the combustor at a microscale from cylindrical walls that are built from a stack of rings held down with a structure of preloaded rods. (Fig. 1) Reagent jet penetration cannot be large. Even considering some global convective processes, the zone with the hottest flame temperatures must be roughly annular in shape, with a width much smaller than the vessel ring radius. (Fig. 2)

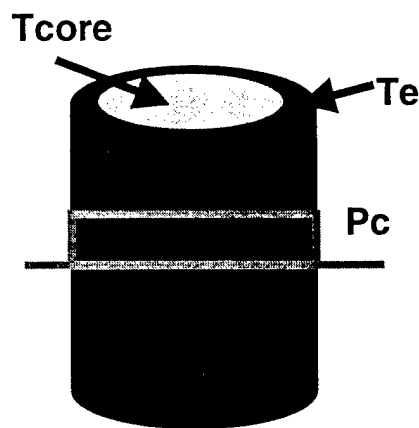


Fig. 2. HYFLAME Two Bin Model

The vessel is empty, so gas under pressure does get blown to the center, namely the core. We will assume that these are uncombusted reagents or expended products. We expect the core to be cooler than the annular flame sheet. The main expulsion of products is a reverse flow between the rings, cleverly designed with an annular throat gap to define a converging diverging nozzle structure. (Fig. 1)

The main influence of the core is to determine the combustor plenum pressure P_c , and thus the stagnation pressure for the nozzle flows. It also provides the density and core temperature history that marches from one time interval to the next.

Implicit above is the idea of a two-temperature vessel. (Fig. 2) Our principal concept is that both zones are characterized by one pressure P_c . The interior flow that is

present, which we do not model, is considered quiescent gasdynamically, despite the obvious temperature gradients. The exit stagnation temperature, commonly T_e , is defined mainly by the thermochemistry and heat losses, as in the prior model. The core temperature, denoted T_{core} , will be defined by P_c and by the number of molecules trapped in the core. The core will be found to be cooler than T_e . Intentionally, the convective processes caused by temperature gradients will not be modeled because of their complexity. Our aim is to emphasize fidelity in the performance of the flame sheet. Thus T_{core} may be a qualitative indicator, but may have a limited physical significance in a real case.

The creation of a core model for HYFLAME is the added complexity previously mentioned. In our solution, we

will need to apply three control volumes with interlinked processes for mass and heat fluxes. (Fig. 3)

HOT ANNULUS

We first model a control volume very similar to that of the previous work. (Ref. 1) Because of the complexity of the description, few equations will appear in this paper, but by illustration, we will describe the elements that go into the analytical modules describing the hot annulus control volume. These elements include the inflow and outflow of mass and energy accompanying reagent and exhaust flow rates. They also include properties of materials that govern mass and heat transfers and the physics of combustion. We envision the annulus of hot gas to be bounded by the vessel wall (the ring stack and end domes).

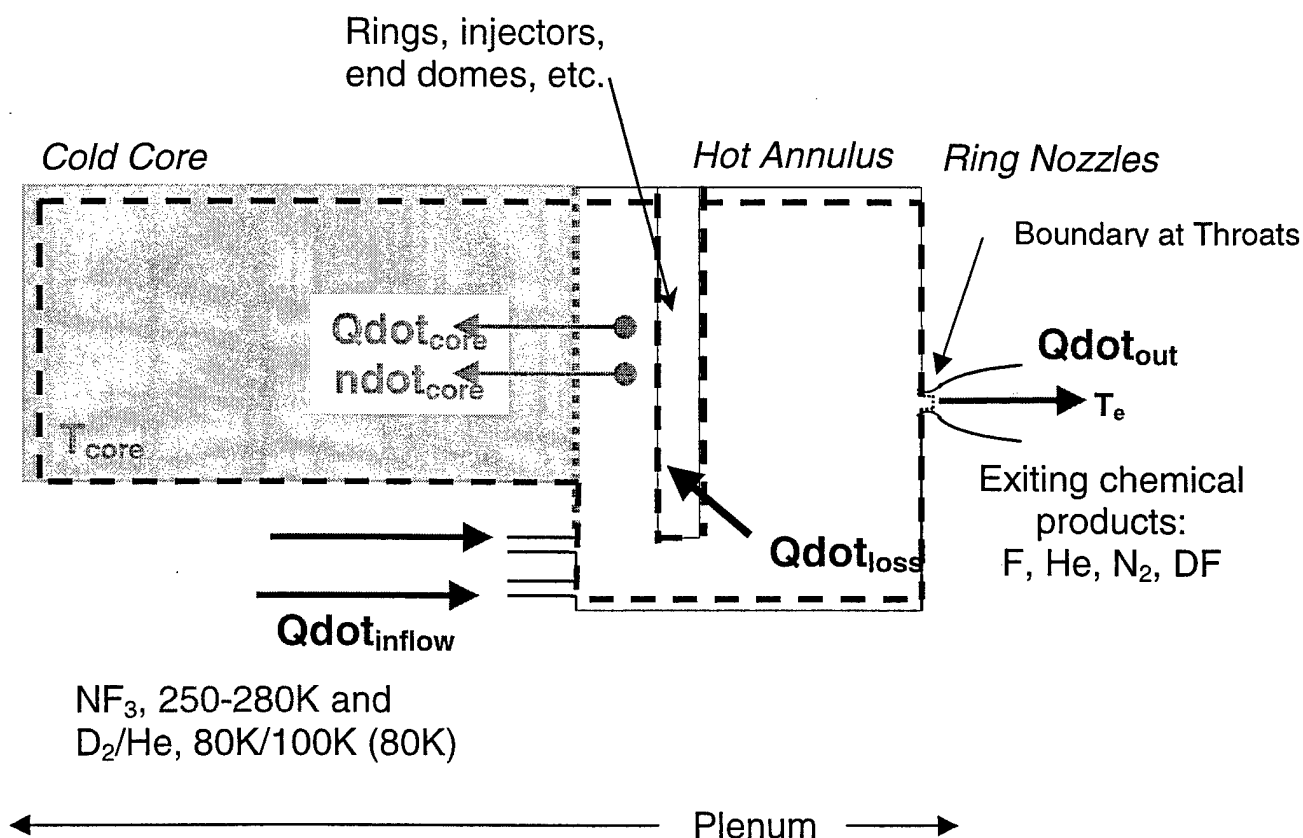


Fig. 3. Functional control volume diagram showing the overall Control Volume (heavy dashed lines) and the three Control Sub-Volumes: *Cold Core, Hot Annulus, Ring Nozzles*.

Inflow. Starting at the lower left corner of the Hot Annulus Volume (Fig. 3), the reagent flow rates during a specific time interval are logged in across the boundary. These reagent molar flow rates are given as a function of time but are assumed constant during the time interval j . The molar flow rates define the mole fractions of reagents, which in turn will allow calculation of the mole fractions of products later. The reagents enter the volume at specified temperatures, which in the case of NF_3 changes as a function of time. The specific heats that reflect the amount of flow enthalpy into the Hot Annulus Volume are also functions of these temperatures. Calculations yield:

- mole fractions for combustion
- \dot{Q}_{inflow} , the heat transfer into the volume as the summation of terms

$$\dot{n}_{i,j} \times c_{p,i}(T_i(t)) \times T_i \quad (3)$$

where \dot{n} is the molar flow rate, c_p is the specific heat and $T(t)$ is the stagnation temperature of the i th reagent.

Losses to the Core. Running clockwise on the diagram of Fig.3, one encounters the dashed boundary along the interface with the Core Volume. Both mass and heat, assumed by conduction, leave the Hot Annulus Volume and are deposited in the Core Volume. As noted earlier, the dynamical processes of fluids are neglected for simplification. Thus the interface is treated as a "rigid" cylindrical gaseous boundary of specified radius. (Fig. 2).

In the j th time interval Δt_j , the number of molecules deposited to the core in steady state through this interface is

$$\dot{n}_{\text{core}} = (\dot{n}_{\text{j-inflow}} - \dot{n}_{\text{j-outflow}}) + N_{\text{j-combustion}} \div \Delta t_j \quad (4)$$

where $\dot{n}_{\text{j-inflow}}$ is the flux of molecules entering the Hot Annulus Volume, $\dot{n}_{\text{j-outflow}}$, the flux exiting the Volume and $N_{\text{j-combustion}}$ is the net number of additional molecules generated by combustion according to the processes we discuss below. Inflow flux is

determined by the inflow of reagents while outflow flux is determined in this model by the one-dimensional steady flow equation for choked flow, and thus by the plenum pressure P_c , stagnation temperature T_e , and throat area A^* . In the perfectly performing system, the net flux to the core would be zero. However, all three governing parameters vary with time, particularly A^* due to thermostructural effects. There is no *a priori* reason why \dot{n}_{j} for the j th internal would be zero. In fact HYFLAME shows that at time-start, \dot{n}_{j} can be significantly larger than zero, thus building up the pressure in the combustor, but as the system approaches thermal equilibrium for longer run times, \dot{n}_{j} does approach zero.

The heat flux \dot{Q}_{core} is determined principally by the enthalpy flux due to the molecular flux \dot{n}_{core} . Heat transfer by thermal conductivity of gases was found to be a small contributor and therefore negligible in changing the thermal content of the core, by estimates. As noted earlier, we are neglecting the convective processes in this model. We take the mole fractions to be those of species in the Hot Annulus, except that F-atoms are assumed to recombine. Heat recovered from the recombination of radical species is booked back into the heat contained in the hot annulus and thus raises the computed stagnation temperature T_e slightly. With these assumptions, molecular weight and specific heat of the core can be defined, and, given a core temperature T_{core} , computed below,

$$\begin{aligned} \bullet \quad \dot{Q}_{\text{(j)core}} &= \dot{n}_{\text{(j)core}} \times c_{pj}[T_{\text{(j)core}}] \\ &\times [T_{\text{(j)core}} - T_{\text{(j-1)core}}] \quad (5) \end{aligned}$$

Net Heat Losses to the Vessel. Moving further clockwise, one meets \dot{Q}_{loss} , heat losses to all parts of the combustor vessel bounding the hot gases.

A careful definition of this part of the Hot Annulus Volume boundary is now necessary to understand the governing equations of these modules. The boundary excludes all the solid surfaces of the combustor, but hugs the strange

contours of the domes, isolation nozzles, and ring array. The parts of the dome areas that are important are those that bound the hot annulus. Between each pair of rings, the boundary penetrates down to the throat gap position of the converging-diverging nozzle structure. This "rubber" boundary is meant to also penetrate each triplet of the thousands of sets in the combustor injection plate, through the rings, distribution logs, and plumbing upstream to the main manifolds feeding reagents to the gain generator, perhaps just downstream of the metering devices. In this way, this Volume cleverly sidesteps the issue of regenerative heating of the reagents in the rings, since this effect is now internal to the Volume. The convective heat losses to the rings that is observed is then a net flux, in fact smaller than the total heat flux loss to walls. Net heat loss is, however, the correct quantity for estimating ring temperature changes and for later computing T_e .

Needless to say, a reasonably accurate portrayal of the vessel heat losses is essential to the success of the model as a predictor. This approach depends heavily on the ability to average key properties and yet preserve some physical fidelity. Undoubtedly, the quasi-steady nature of the process (except very close to time-start), the large spatial scales of the vessel and even nozzle structure relative to the microscales of combustion, and the completeness of the chemical processes at these time scales have helped immeasurably in fostering the applicability of this model. As previously noted, we emphasize that this model is to be used for insight.

The analyses for this module are similar to that previously reported¹. As suggested in Fig. 1, the principal heat losses in the combustor would be by convective processes. There might be a secondary effect from radiative processes because of a high stagnation temperature in the plenum. It is difficult to scale these processes to the end domes of the cylindrical vessel. Firstly, the fluid flow processes there are, as yet, ill-defined. Secondly, in contrast to the ring nozzle array making up the sides of the cylindrical vessel, the domes are water cooled, and so actually are held at constant temperature, 300K.

We describe the net heat energy lost to the vessel side wall (the rings) as follows:

$$\dot{Q}_{\text{loss,ring}} = [\text{heat flux loss}] - \dot{Q}_{\text{regen}} \quad (6)$$

Where

$$[\text{heat flux loss}] = [\text{convective}] + [\text{radiat}]$$

$$[\text{convective}] = \dot{Q}_{\text{regen}} + \bar{h} \times A_{\text{vessel}} \times (T_e - T_{A1})$$

$$[\text{radiative}] = E \sigma A_{\text{vessel}} \times (T_e^4 - T_{A1}^4)$$

As noted above, this conveniently cancels \dot{Q}_{regen} , heat flux transferred into the reagents, out of the problem. This difficult-to-estimate term is important if one seeks to know the flame temperature (sometimes denoted T_i , see for example Ref. 2) at the triplet zone. T_e represents the average plenum temperature to be defined below by the thermochemistry. T_{A1} is the average vessel ring wall temperature., and A_{vessel} is the simplified side wall area, considered a cylinder at vessel radius. The net convective term, less regenerative transfer, resembles a convective heat transfer term if T_e approximates the recovery temperature of the gas, typically for turbulent subsonic boundary layers actually about 0.8-0.9 T_e . T_{A1} is supposed to be representative of the surface temperature at

the point of heat transfer. Since the ring is regeneratively cooled, T_{A1} is in fact probably a few degrees lower than the actual surface temperature that should be used. Modeling of the relative temporal variation, however, is expected to be quite good. So \bar{h} becomes a kind of spatially averaged convective heat transfer coefficient. For the radiative term, by the same token, E is a kind of spatially average emissivity, which we take to be the same for the gas as for the ring for simplicity and lack of better data, and σ is the Stefan Boltzmann constant.

Both \bar{h} and E need to be anchored by fitting empirical observables such as P_c and ring temperatures as a function of time for the identical vessel for which predictions for future testing are to be made. This approach using the

data of Alpha Laser tests HL910 and 911-003 will be discussed later.

The heat transfer expression $\dot{Q}_{\text{loss domes}}$ for loss to the domes or end caps is very similar to Equation 6 except in the following respects. T_{Al} is replaced by the constant temperature, 300K, because of cooling by water. A_{vessel} is replaced by the areas of the intersection of the hot annulus with the domes, which we take to be approximately flat caps. Term $\bar{h}_{\text{bar-domes}}$ is taken arbitrarily to be 0.5 $\bar{h}_{\text{bar-rings}}$. We contend that flow at the dome surface has perhaps half the velocity, on the average, as that entering a nozzle throat. An actual convective heat transfer coefficient is proportional to velocity to the 4/5th power, all other gas properties being the same. In any case heat loss to the domes is around 10% of the total loss from the gas, so that the large uncertainty yields a negligible impact.

T_{Al} , the average ring temperature, is deduced from the heat content of the aluminum structure using Eqn. 6 and :

$$\dot{Q}_{\text{loss rings}} = \rho V_{\text{rings}} C_{p-\text{Al}} [T_{j\text{Al}} - T_{(j-1)\text{Al}}] \div \Delta t \quad (7)$$

where the temperature of the aluminum ring set in time interval j is raised relative to that of the prior time interval $j-1$. Term ρV_{rings} where V_{rings} is the volume of the ring stack, can also be given by the known mass of the rings, and $C_{p-\text{Al}}$ is the specific heat of aluminum. In reality, the temperature distribution across the ring cross section must be very non-uniform due to regenerative cooling. Consequently, T_{Al} may not be representative of any specifically measured temperature, as we shall see, but may at best reflect the temporal trends of the observations.

To recap, this module of the model allows us to estimate

- $\dot{Q}_{\text{loss rings}}$, heat loss to the stack
- $\dot{Q}_{\text{loss domes}}$, heat loss to the caps
- T_{Al} , average temperature of the stack.

Throat Gaps and Exit Flows. Moving further clockwise around the Hot Annulus Control Volume boundary, we finally arrived at the nozzle, symbolic of the 25 annular nozzles formed by the aluminum rings as depicted in Fig. 1. As we have discussed ¹, the expansion of the ring cross sections due to heating tends to close the throat gaps as a function of time. Plenum pressure P_c and total molecular flow \dot{n}_{outflow} through the nozzle array will be affected temporally.

Structurally, the Alpha gain generator is assembled in such a way that the center planes of the rings are literally fixed in space, relative to a stable ground reference plane. Thus an expression can be written to model the material growth of neighboring rings from both directions orthogonal to the gap, which narrows the gap. Total area A^* of the gaps is given by:

$$A^* = N\pi D\epsilon x (1 + \text{CTE}(T_{\text{Al}} - 250)) \{1 - [2(l/\epsilon)\text{CTE}(T_{\text{Al}} - 250)]\} \quad (8)$$

where N is the number of gaps, 25, D is the diameter of the rings, ϵ is the starting gap width between two pre-cooled rings at 250K, and CTE is the linear coefficient of thermal expansion of aluminum. Term l/ϵ is very slowly varying with time in these cases where l is the initial geometric half span across a ring cross section from its center line to the throat. Term l/ϵ is therefore taken as a constant.

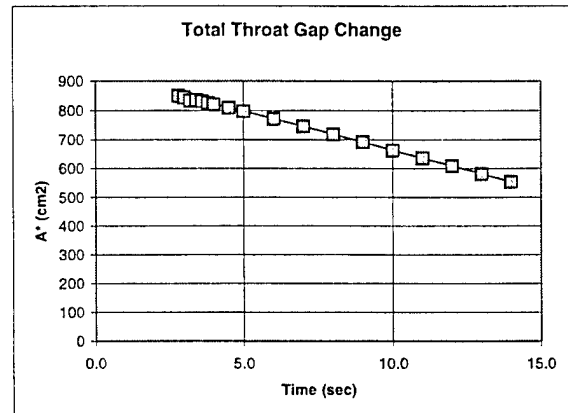
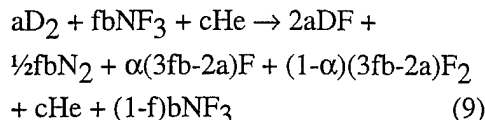


Fig. 4. Typical result: A^* as $f(t)$ for HL911-003 case

Hot Annulus Interior. Having traversed the boundary of the control volume, we have

identified the major mass and heat transfers. Arbitrarily, we take the width of our Hot Annulus as 10 cm. Description of combustion, a major source of mass and energy, is governed by the well-known chemical balance:



Free parameter, fraction f , has been added to simulate incomplete combustion at the earliest times after time-start when the assumption of complete NF_3 dissociation can drive deduced Te well below 1350K, estimated lower limit for complete NF_3 dissociation from thermodynamic equilibrium considerations. We will define a Te_{min} , below, which we assume that no NF_3 dissociation takes place, and that will set f between 1.0 and 0. Parameters a , b , and c are mole fractions deduced from incoming flows. The heats of formation as $f(Te)$ of species in Eqn. 9 are required to compute the net heat flux $Qdot_{thermochem}$ generated from thermochemistry.

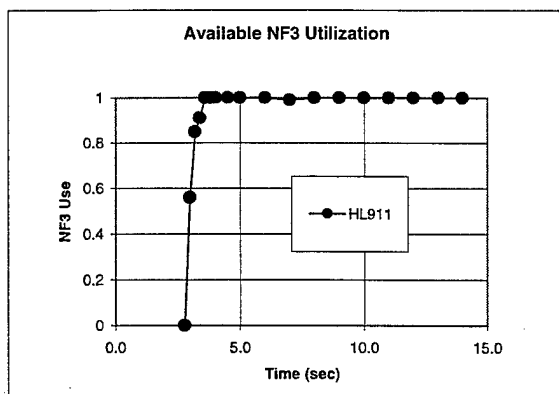


Fig. 5. Parameter f for HL911-003 case for $Te_{min}=1350^{\circ}K$

In this module for modeling the gaseous interior of the Hot Annulus, the main objective is the computation of Te , the plenum or average stagnation temperature of the mixture exiting through the nozzle throats. The value of Te affects the heat flux loss (Eqns. 5 and 6), indirectly the vessel temperature T_{A1} (Eqn. 7),

and therefore A^* (Eqn. 8). Te also determines the degree of dissociation of F_2 , α , and Pc .

$$Qdot_{out} = Qdot_{inflow} - Qdot_{gas\ loss} + Qdot_{thermochem} \quad (10)$$

$$Te = Qdot_{out} \div ndot_{out} \times Cp_{out} \quad (11)$$

Where Cp_{out} is weakly a $f(Te)$ and must be computed, given the mole fractions and $Cp_i(Te)$ of products i . The various linkages and weak nonlinearities in Te are best treated using a converging iteration of linked equations. We have for loop 1. Cp_{out} , then loop 2, α and readjustment to $Qdot_{thermochem}$, and loop 3, readjustments to $Qdot_{out}$ due to $Qdot_{gas\ loss}$. Fewer than 4 iterations will usually generate better than 1% agreements in key solved parameters such as

- Te
- α , degree of F_2 dissociation.

NOZZLE FLOW

The Nozzle Control Volume can be taken in each of the 25 annular nozzles, from the throat gap to nozzle exit plane (NEP) and bounded by the contoured walls of the hypersonic nozzle. Given the combusted gas mixture properties from above and a computation for Te , Pc is given by the one dimensional steady flow expression for choked flow, for jth interval:

$$Pc = f_{ndot} ndot_{c-out} \times \sqrt{W Ro Te} \div A^* f(\gamma) \quad (11)$$

where W is the mixture molecular weight, Ro is the universal gas constant, and $f(\gamma)$ is the usual function of the ratio of specific heats γ . Notice that an artificial fraction f_{ndot} has been introduced to facilitate a successful simulation based on anchoring experimental observations of Pc , especially around time-start. Estimated together with f for a given observed Pc , say for HL910, a schedule for $f_{ndot}(t)$ is generated to use in predicting future test flows such as HL911. It is found to reach 1.0 within a few seconds after time-start, similar to Fig. 5 for f . Successful use of f and f_{ndot} to predict Pc is given in Fig. 6

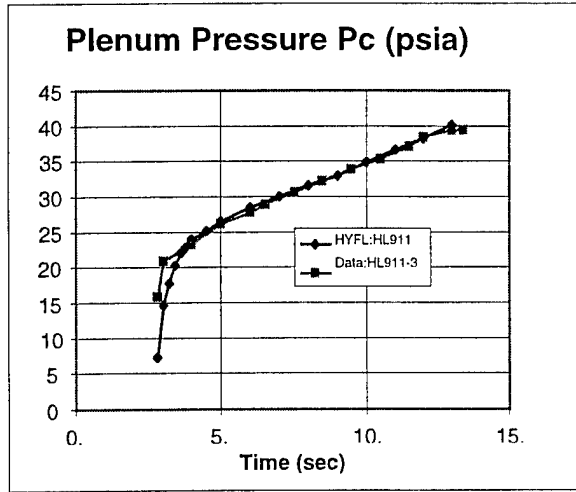


Fig. 6. Fitting the P_c curve of HL911-003

It can be seen that both time dependent slope and absolute values are in excellent agreement except very near time-start.

Part of the P_c discrepancy is due to what is surely a radially and azimuthally non-uniform start up. Our use of somewhat arbitrary parameters f and \dot{f}_{ndot} may also contributed. Finally, we have not yet modeled the effects of the slug of fluorine used to ignite the ox/fuel mixture initially.

However, the use of f , \dot{f}_{ndot} and T_{e-min} are important in simulating the combustion and vessel history for the longer times.

We have made (Ref. Eqn. 4):

$$\dot{n}_{j-outflow} = \dot{f}_{ndot} \times \dot{n}_{j-c-out}, \text{ and}$$

$$\dot{n}_{j-c-out} \equiv \dot{n}_{j-inflow} + N_{j-combustion} \div \Delta t$$

namely, not all the molecules created in combustion are ejected immediately.

From kinetic analysis, we always find about 1% recombination of F-atoms into F_2 during the 1-D flow down the HYWN nozzle structure to the nozzle exit. That effect will be included in our computation of degree of dissociation and F-atom flow rate.

CORE VOLUME

Our Core Control Volume models the interior of the cylindrical combustor, within which P_c is assumed the same and that thermodynamic equilibrium prevails. The resultant gas mixture is assumed to be a perfect gas with the same species molar fractions as those in the counterpart Hot Annulus, except that F atoms have recombined, releasing heat back into the hot annulus. During time interval Δt_j , Eqn. 4 gives the number of molecules added to the core, and Eqn. 5, the heat flux to the core. The current model shows that at longer combustor times, the core mass and heat transfer effects were essentially negligible, thus justifying the utility of the previous work¹ while illustrating the essential role of core behavior early, at time-start.

With the assumption that core pressure and hot annulus pressure are both P_c , the perfect gas law gives

$$T_{core} = P_c \div (N_{core}/V_{core})k \quad (12)$$

where N is number of molecules in the core, " V_{core} " is core volume and k is the Boltzmann constant. N_{core} is defined by Eqn. 4 and

$$N_{core-j} = N_{core-(j-1)} + \Delta t \times \dot{n}_{j-core} \quad (13)$$

Although clearly linked to Eqn. 12, Eqn. 13 also links to Eqn. 11 through flow rate term $\dot{f}_{ndot} \times \dot{n}_{j-c-out}$. Meanwhile heat transfer expressions also define T_{core} as follows:

$$T_{core} = \{Q_{core}(j-1) + \Delta t \times Q_{dot-core-j}\} \div W_{core-j} \times N_{core-j} \times C_{p-core-j} \quad (14)$$

with Q_{core} , the heat content in the core gas in the prior interval, $Q_{dot-core}$ given by Eqn. 5, W the molecular weight of the core gas mixture and C_p the heat capacity, a function of T_{core} . A small iteration on Eqn. 14 is needed for a consistent solution. But Eqn. 14 is linked clearly to Eqns. 12 and 13. The simultaneous solution for T_{core} , and P_c , N_{core} , \dot{f}_{ndot} , requires iteration as well. Fortunately, the perturbing terms Eqns. 13 and 14 are small, especially in time regions much later than those at time-start, so the solution for T_{core} approximates that of Eqn. 12 and that for P_c is defined largely by Eqn. 11. A typical

calculation of T_{core} is shown in Fig. 7. It is not surprising to see that T_{core} values are smaller than those for T_e , namely the core is cooler. It is difficult, however, to quantify the behavior further with HYFLAME because the core is crudely portrayed, and fluid dynamics due to the obvious temperature gradients are not included.

ANCHORING PARAMETERS

In this "insight" model we have created a number of parameters ($hbar$, E , f , f_{ndot}) to facilitate the simulation of observed combustor performance. These parameters are based on aspects of physics insight governing probable behavior in a cylindrical combustor. However these parameters are not derived from first principles and must be anchored. (namely fitted using observables). In Fig. 8, we suggest the process using fits to HL911-003 Pc data. We have also used HL910 data as well to derive the most consistent set of $hbar$ and E parameters.

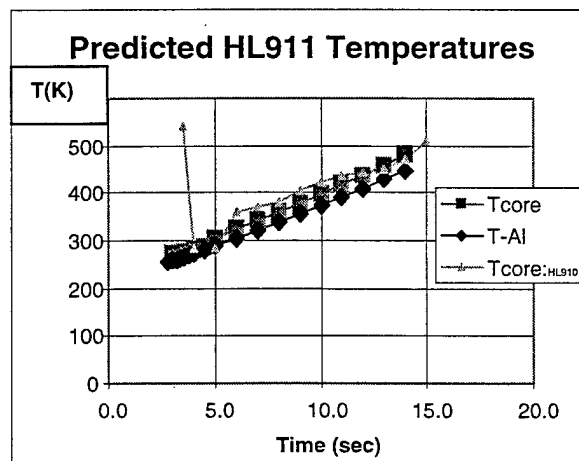


Fig. 7. Typical T_{Al} , T_{core} calculations, HL 911-003

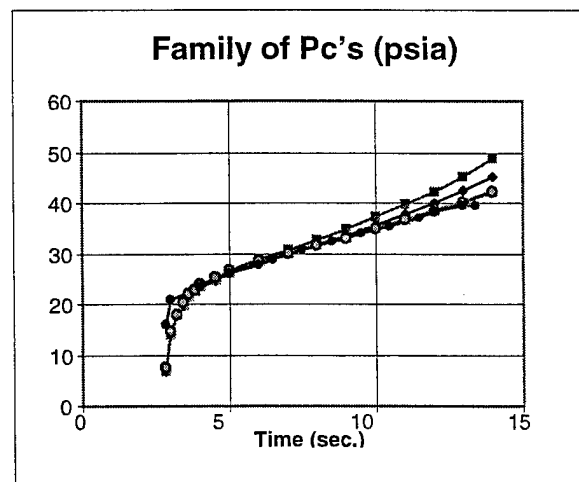


Fig. 8. Families of HYFLAME Pc curves simulating HL911-003, to illustrate parameter anchoring.

◆ ($hbar=0.04$, $T_{e-min}=1400$, $E=1.0$), ■ ($hbar=0.05$, $T_{e-min}=1400$, $E=1.0$); ▲ ($hbar=0.05$, $T_{e-min}=1450$, $E=0.2$); ○ ($hbar=0.05$, $T_{e-min}=1350$, $E=0.2$); and ● (HL911-003 Pc data).

In general, we sought values of $hbar$ as large as possible to match Alpha Laser ring thermocouple data with our T_{Al} calculations. Pc is insensitive to T_{e-min} variations. Too-high values of $hbar$ and E tend to cause a nonlinearity in Pc at longer times, clearly in the wrong direction. (Fig. 8) Thus we chose

$$hbar \leq 0.05 \text{ watts/cm}^2\text{K and } E \leq 0.2.$$

For a set of parameters, HYFLAME enables us to estimate key parameters of combustor performance not readily accessible by direct measurement or data analysis from a test. Example are the principal results sought from this insight model, the apparent F-atom flow rate generated by the combustor and its companion variable, the degree of dissociation. A set of anchored parameters also permits the prediction of the performance of the very same combustor as a function of time in future tests. One such effort will be an attempt to forecast the F-atom flow rate of HL912.

PRINCIPAL RESULT

Once T_e is computed, there follow computations for degree of dissociation, the mole fractions of products, and $ndot$ -outflow. We can then compute the F-atom flow rate in moles per second from all 25 annular nozzles. (Fig. 9).

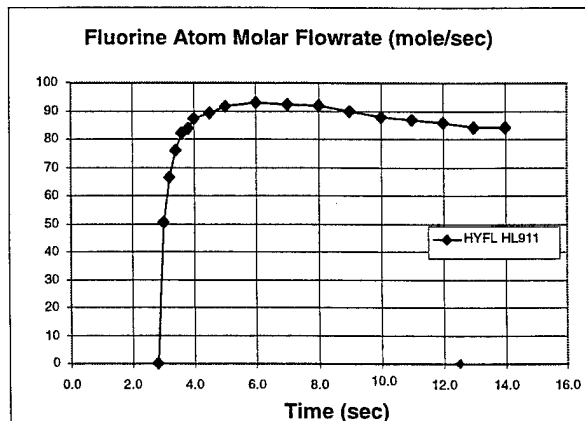


Fig. 9. F-Atom Flow Rate computed from HYFLAME as a function of time. ($\bar{h}=0.05$ watts/cm²K, $E=0.2$, $T_{e-min}=1350$ K).

The HYFLAME computation of F-Atom flow rate suggests that the laser would probably experience equal or slightly better laser performance at earlier flow times for this flow condition, nominally a $\dot{m}F/A$ condition of 0.25 kg/m²-sec. As we can see in Fig. 11, peak F-atom flow rate actually occurs at lower degrees of dissociation. This model forecasts that the flow rate declines at later times even though the degree of dissociation continues to rise. This effect is mainly due to the A* throats closure due to thermal heating and the consequent dropping of $\dot{m}_{outflow}$ as a function of increasing time. (See Eqn. 11).

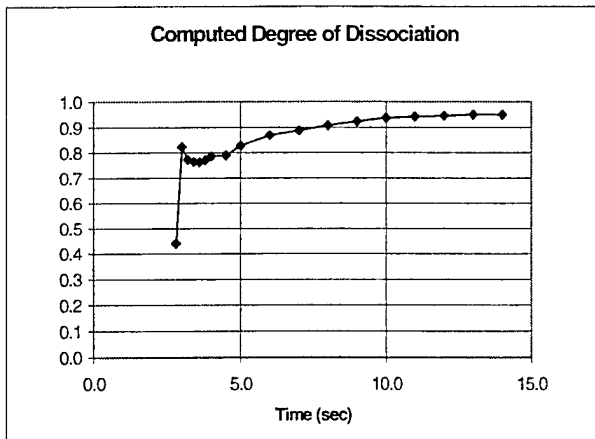


Fig. 10. Computed degree of fluorine dissociation α For the HL911-003 flow conditions.

For this HYFLAME run simulating HL911-003, the degree of fluorine dissociation reaches a plateau of 0.94 at shutdown (Fig. 10) while T_e at that same time is computed to be 1610°K. T_{Al} computations exhibit a similar trend slope to Alpha ring thermocouple data. T_{Al} ending temperature is around 450°K while most of the Alpha data indicate temperatures just above 500°K. However, *relative* temperature changes in the aluminum rings are synthesized in the model. Model starting temperature is 250°K, while Alpha ring data starts around 270-280°K. Further, computed T_{Al} reflects a global average across ring cross section and the part is regeneratively cooled. Alpha data, on the other

hand, is geared toward sampling the regions of high heat transfer. Thus the end temperature disagreement may not be a serious discrepancy.

Average heat loss to rings and domes computed by HYFLAME is around 5×10^6 watts while data analysis from the Alpha thermocouple data suggests an average over time around 5.2×10^6 watts.² However, a current key discrepancy is that HYFLAME predicts a slight increase in \dot{Q}_{loss} in time, while Alpha results indicated about a 15% to 20% decline. One easy modification in HYFLAME would be to make \bar{h} time-dependent, but the lack of sensitivity to anchor data may preclude the ability to verify and therefore implement the modification.

CLOSURE

This work has shown the development of an insight model that is successful in simulating many of the features, characteristics, and behaviors of a cylindrical combustor used as a chemical laser gain generator. The inherent model architecture and its relative simplicity have helped to reveal the many highly linked physical intricacies among the various internal parts of the combustor, highlighting particularly the role of the cooler core in governing time dependent performance. The model suggests that good laser performance may occur at much earlier cavity fuel turn-on times in a combustor flow condition such as HL911-003.

ACKNOWLEDGMENTS

Special thanks to Dr. Sherwin Amimoto who raised many of the questions and contributed to physical insights in the model. We also thank Drs. Robert Waldo, Pete Lohn, Dan Novoseller, TRW Space and Defense, and Gary Morr, SAIC for helpful discussions and data. We also thank Capts. Dean Fitzgerald and Matthew Zuber, of SMC/TL, Mr. Joseph Jackson, Ms. Lorraine Ryan, of TRW Space and Defense, and Dr. David Johannsen, The Aerospace Corporation for their continued interest in this work.

This work was performed under SMC Contract F04701-00-C-0009. Space and Missiles Systems Center does not endorse nor disavow these findings.

REFERENCES

1. Munson A. Kwok and Sherwin Amimoto, "Modeling HF Gain Generator F-Atom Flows." 31st AIAA Plasmadynamics and Lasers Conference, 19-22 June 2000, Denver, CO. AIAA 2000-2497, 16 pp.
2. Lorraine Ryan, Bernie Bendow, and George Clark, Jr., "Alpha Laser Test Results: HL910 and HL911." 32nd AIAA Plasmadynamics and Lasers Conference, 11-14 June 2001, Anaheim, CA. AIAA 2001-2867.



2350 E. El Segundo Boulevard
El Segundo, California, 90245-4691
U.S.A.